

Research Paper

Robust Scheduling of Unbalanced Microgrids for Enhancing Resilience by Outage Management Strategy

Shirkooh Panjeie¹, Ahmad Fakharian¹, * , Mostafa Sedighizadeh² , and Alireza Sheikhi Fini³ 

¹ Department of Electrical Engineering, Qazvin Branch, Islamic Azad University, Qazvin, Iran.

² Faculty of Electrical Engineering, Shahid Beheshti University, Evin, Tehran, Iran.

³ Department of Power Systems Operation and Planning, Niroo Research Institute, Tehran, Iran.

Abstract— Microgrid operators (MGOs) try to restore as much demand as possible when they are faced with electrical power outages corresponding to extreme events. This work suggests an outage management strategy (OMS) to improve microgrid resilience by using two optimal actions that are distribution feeder reconfiguration (DFR) and scheduling of the distributed energy resources (DERs). Later happening a line fault, the radial network topology is determined by the proposed model using an evaluation of the incidence matrix. The presented work handles the uncertain behavior of non-dispatchable DERs and the electrical loads which model by the robust optimization approach. To expand the flexibility of the proposed model, the demand response program (DRP) is treated as the curtailed demand. The aim of optimization is the minimization of the total cost for dispatchable DER operation and electrical load decrease. The recommended robust linear problem (RLP) model is simulated by the CPLEX solver in GAMS software. Applying the suggested model in the 69-bus unbalanced test system demonstrate that the proposed model averagely decreases total operation cost and execution time by 10.62% and 22.23% on all scenarios in comparison with the de-deterministic model.

Keywords—Distributed energy resource, distribution feeder reconfiguration, resilience, robust optimization, outage management strategy.

1. INTRODUCTION

1.1. Motivation

Recently, the resilience concept has been introduced in the electrical power system that shows the efficacy of an electrical power systems to adjust and restore from important electrical power outages corresponding to accidents, cautious attacks, or natural catastrophes [1, 2]. In these years, major economic losses have happened due to electrical power outages in DNs and MGs. According to statistical data, weather events are an important reason for electrical power outages in the DNs of the U.S. [3]. Weather events and other extreme disturbances may lead to several line outages and faults and crews need numerous hours and even more than one day for repairing actions and restore faulted equipment [4, 5]. During the outage period, minimization of the energy not supplied and consequently minimization of the penalty cost pertaining to load shedding is the desired goal for electric utilities. The above-mentioned cost is an important quantity of DN resilience [6].

According to the literature [1], resilience can be enhanced by three significant approaches. The first approach is to increase the strength of DN poles in main and vital lines so that their fracture

probability decreases during severe climate events [7, 8]. The second is DFR to restore the loads at islanded feeders by changing the route of supplying electrical power during line outages faults [9, 10]. The third is to use DERs that are dispatchable and non-dispatchable generations as well as ESSs [11, 12]. This paper presents a robust modeling for enhancing the DNs resilience considering optimal management of DFR and DERs.

1.2. Literature review

Concerns about improving resilience have been addressed by literature from a different point of view. [7] proposes a tri-level model for minimizing energy not supplied and the cost of load reduction under severe weather. Authors of [7] continued their work in [13] by proposing a stochastic model based on two hardening actions that are to increase the strength of DN poles and utilize backup DGs. Though, it can be noted that [7, 13] didn't take into account DFR. [8] introduces a model to optimize the strengthening plan, but, the proposed model is too conservative due to a small probability of a worst-case scenario that is used in this paper. [14] uses an imperialist competitive algorithm to reconfigure the DN with the goals of minimization of electrical power loss and improving reliability. [9] presents an effective model for the DFR of DNs. The objectives are to minimize real electrical power losses, the deviation of voltage profile, the branch current constraint violation, and switching operations number. Though, the optimal operation of different technologies of DERs is not involved in [9, 14].

[11] classifies the operation of a DN into two modes that are self-healing and normal modes. In the self-restoration mode, the faulted part of the DN is divided into self-supplied MGs to lessen the number of impacted loads. [12] proposes an optimization model for outage management to contribute DERs among MGs.

Received: 04 Aug. 2022

Revised: 31 Oct. 2023

Accepted: 01 Nov. 2023

*Corresponding author:

E-mail: ahmad.fakharian@qiau.ac.ir (A. Fakharian)

DOI: [10.22098/joape.2024.11267.1841](https://doi.org/10.22098/joape.2024.11267.1841)

This work is licensed under a [Creative Commons Attribution-NonCommercial 4.0 International License](https://creativecommons.org/licenses/by-nc/4.0/).

Copyright © 2025 University of Mohaghegh Ardabili.

[15] develops an outage management frame-work for minimizing the loss of demand in emergency circumstances taking into outage duration vagueness consideration. Though, this reference considers active electrical power as the objective of optimization, and voltage constraints are ignored. It can be noted that the DFR is not considered in [12, 15]. [16] presents an algorithm that divides the DN into numerous MGs after the occurrence of line faults. The algorithm presented by this reference wants to maximize the restored loads in each MG. [17] proposes a restoration mechanism to find the post-restoration topology and schedule the vital load. Also, [18] suggests an optimal switching operation to restore the DN. In [19], a service restoration scheme via DFR is formulated as a mixed-integer second-order cone programming problem. [20] develops a resilience improvement model based on the optimal siting of remotely controlled switches for minimizing load shedding in post-event duration. [21] suggests a methodology based on complex network theory to assess the planning and operational resilience of DNs under extreme events and determines the withstand competence of the electrical network. [22] proposes a framework for resilience improvement in pre-attack and post-detection stages using three techniques that are optimal allocation of DERs, optimal intelligent electronic devices diversification, and optimal DFR. [23] suggests day-ahead resilience evaluation is based on a multi-stage approach that calculates the probabilities of failure of each line and determines the most vulnerable ones and then does the optimal DFR considering non-dispatchable RESs to minimize the loss of load during the windstorm. [24–26] present joint optimal DFR and DER scheduling. The weakness of these references is to be degraded the life of switches due to the number of switching. To sum up briefly, the management mechanisms in [11, 12, 15] and in [16–19] supply vital demands by making suitable utilization of DERs. These references assume that the capacity of DERs is uniformly sited in the DN and the infiltration level of DERs is adequate to supply the adjacent demand. Conversely, given a region of the DN has severely loaded but a small to a modest infiltration level of DERs has been installed in it, it is challenging to form multiple self-supplied MGs inside this region. To solve this weakness, [27] presents an outage management strategy (OMS) to improve DN resilience for a small to a modest infiltration level of DERs. It can be noted that [27] considers PDF of indeterminate parameters that are DERs generation and loads and if there is no adequate information about the PDF of indeterminate parameters, the proposed model will fail to obtain optimal results.

1.3. Contributions and organization

Based on the formulation proposed by [27], an OMS is proposed by this paper in order to improve the resilience of the unbalanced DN equipped with a small to a modest penetration level of DERs. The proposed OMS comprises post-fault DFR and optimal arrangement of various technologies of DERs including non-dispatchable or dispatchable in MG. Despite [27], this work undertakes that there is no satisfactory information about the PDF of indeterminate parameters including non-dispatchable generations and demands. Therefore, it uses a robust optimization method to model vagueness. The aims of the presented work are as follows:

- Reformulating the model proposed by [27] as a robust optimization-based model,
- Sensitivity analysis of objective functions against variation of the uncertainty parameter, and
- Applying the proposed model on unbalanced DNs.

The paper is continued as follows: Section 2 states the problem formulation for the proposed OMS. At that time, Section 3 redevelops the anticipated model handling the robust optimization vagueness modeling. Next, the solution algorithm and flowchart are stated in Section 4. Later, Section 5 precisely discusses simulation outcomes and results. Last, Section 6 depicts the paper's conclusion.

2. PROBLEM FORMULATION FOR PROPOSED OMS

This section elucidates the definition of optimal OMS and assumptions as well as objective function as well as the restrictions as follows:

2.1. Optimal OMS

It is clear that during severe weather events, line faults might island one or multiple parts of the feeders of the MG. Of course, crews of MGs can restore islanded loads by closing tie switches and supplying these loads via another feeder [28]. This new MG topology is kept for numerous hours till the faulted lines are effectively mended. In this time slot, there are several achievable DFRs that might guarantee the radiality of the MG. Regarding new DFR can cause overloading of lines, consequently, the dispatchable DERs are turned on to feed the local demands and some interruptible demands are disconnected. However, both arrangements have an operating cost, including fuel costs and incentive expenditures for consumers. Consequently, a practicable topology that leads to minimal cost is considered the optimal OMS.

2.2. Assumptions for the optimization model

Numerous assumptions are considered for the suggested optimization model as follows:

- MGs have numerous SSs and TSs which can be remotely controlled. Moreover, there are several fault detectors that can effectively locate the faulted lines.
- The MG is supplied by the upstream grid within the normal operation. Also, the upstream grid is not affected by extreme weather and it normally works during events [27].
- For simplicity, the non-dispatchable DERs include PVs and dispatchable DERs comprise MTs. It can be noted that the electricity price of MTs is usually more than the upstream grid. It is assumed that DERs have a unity power factor and the operation cost of PVs is considered equal to zero.

2.3. Objective functions

The proposed OMS has an objective function as Eq. (1) that is operating cost within the time slot of an electrical power outage. The objective function includes two parts that are operation cost of MTs and incentive expense for demand reduction. It can be noted that during extreme climate situations, supplying demands is more significant than decreasing the operation cost. Nevertheless, the operation cost in Eq. (1) presents a measure of the unsupplied electrical energy taking into account weighting factors of various kinds of demands.

$$\text{Cost}(G(k)) = \min \left[\sum_{t \in T} \Delta t \times \left(\sum_{g \in N_{MT}} C^{MT}(g) \times \sum_{\varphi \in N_{ph}} P^{MT}(g, t, \varphi) + \sum_{d \in N_L} C^L(d) \times \sum_{\varphi \in N_{ph}} \Delta P^L(d, t, \varphi) \right) \right] \quad (1)$$

2.4. Topological limitations of the MG

Having a radial topology is one of the essential requirements after DFR. This paper considers a rank-based constraint to choose the radial topologies.

A) Requirements for the radial topology

Considering a model of directed graph $G(N_{bus}, N_{br})$, a tree is expressed as a connected graph without cycles. It can be noted that the MG has a tree topology which is named a radial topology in power system analysis. Equal to the number of all of the lines and buses, the algorithm of the depth-first-searching is used [27]. In the normal operation of the MG, the positive direction of N_{br} is considered the power flow direction. The bus-line incident matrix

E of the graph G can be formed. The elements of E that are e_{il} are considered as follows [27, 29]:

$$e_{il} = \begin{cases} 1 & \text{if bus } i \text{ is the "from bus" of line } l \\ -1 & \text{if bus } i \text{ is the "to bus" of line } l \\ 0 & \text{if bus } i \text{ is not connected with line } l \end{cases} \quad (2)$$

Lastly, the matrix E is formed as $E = [e_1, e_2, \dots, e_{N_{br}}]$, where e_l is l -th column of matrix E . Regarding graph theory, the essential and adequate conditions for guaranteeing the radial topology of a MG are as follows [27, 29]:

- If E is a connected graph on N_{bus} buses, then $rank(E) = N_{bus} - 1$.
- The number of lines in a tree with N_{bus} buses is $N_{bus} - 1$. On the contrary, a linked graph with N_{bus} buses and $N_{bus} - 1$ lines is a tree.

While faults happen in lines, MGO should form an optimal DFR such that the radial topology of MG is preserved. Of course, under this new topology, the operation cost during electrical power outage including the cost of MT output and cost of load re-duction should be minimized. Consequently, the MGOs should close numerous TSs and open numerous SSs until the disconnected feeder is linked to other feeders. Based on the analysis done in [27], the essential and adequate conditions to preserve the radial topology are written as follows [27]:

$$\sum_{l \in N_{br}} s_l = N_{bus} - 1 \quad (3a)$$

$$s_l = 0 \quad \forall l \in N_{br}^{fault} \quad (3b)$$

$$\acute{e}_l = e_l \times s_l \quad \forall l \in N_{br}, \forall \acute{e}_l \in \acute{E}, \forall e_l \in E \quad (3c)$$

$$rank(\acute{E}) = N_{bus} - 1 \quad (3d)$$

Eq. (3a) guarantees that the total number of closed lines is the same as the number of buses (without considering the slack bus). It can be noted that s_l equals 1 if line l either doesn't have remote-controlled switches or operates in normal conditions. Eq. (3b) expresses that the protection relay opens the faulted line l . Also, the matrix $\acute{E} = [\acute{e}_1, \acute{e}_2, \dots, \acute{e}_{N_{br}}]$ is produced by Eq. (3c) after the DFR. Finally, the under-study graph is a connected graph if Eq. (3d) is met.

B) Pre-defined DFR structure

Regarding Eq. (3a), the MGO will close p TSs ($p \geq q$) and open $p - q$ SSs if q lines are faulted. While the constraint Eq. (3d) should be satisfied by the new topology. Within the process of load restoration, the proposed OMS should prevent too many numbers of switching actions. Consequently, it is assumed that $0 \leq p - q \leq 1$ in this paper. Earlier executing the OMS, the MGO should make a list of DFR structures for the expected fault in each area. The set of DFR structures is represented by Eq. (4a) and each topology is denoted by Eq. (4b) which is a vector of states of line switching as follows [27]:

$$G = [G(1), G(2), \dots, G(N_G)] \quad (4a)$$

$$G(k) = (s_1, s_2, \dots, s_{N_{br}}) \quad (4b)$$

To sum up briefly, the suggested DFR approach is expressed in the following steps.

Step 1: Classifying the entire MG into numerous areas and considering a number for each of them. To define an area, the following procedure is done: scan all buses from the substation or slack bus to the bus that is in the end of feeder, if there is more than one child bus for a bus, after that scan from each child bus to the downstream side. To conclude, all of the buses from the preceding child bus to the end bus are taken into account as an area.

Step 2: Assuming that a single contingency happens in an area, provide a list of all DFR structures by varying the TSs and SSs states. It can be noted that each area of the real MG has one or two remotely controlled SSs [24, 30]. Moreover, at least one TS which is linked to the faulted area should be closed in each topology $G(k)$. Regarding this note that with closing two TSs for a single-contingency line outage, a loop is made, consequently, one SS should be opened in this loop.

Step 3: Assuming that a double contingency happens in any two areas, a possible DFR topologies list should be generated by succeeding in a way like Step 2. It is worthwhile to note that a similar procedure is used for generating a list of configurations for three-line faults.

The fault detector will send the necessary information to the MGO if a line outage happens. Afterward, the faulted area is determined by MGO who requests the list of the topologies in the database presented in Fig. 1. Finally, the topologies that can meet Eq. (3d) are chosen for optimal DER scheduling and operation cost evaluation.

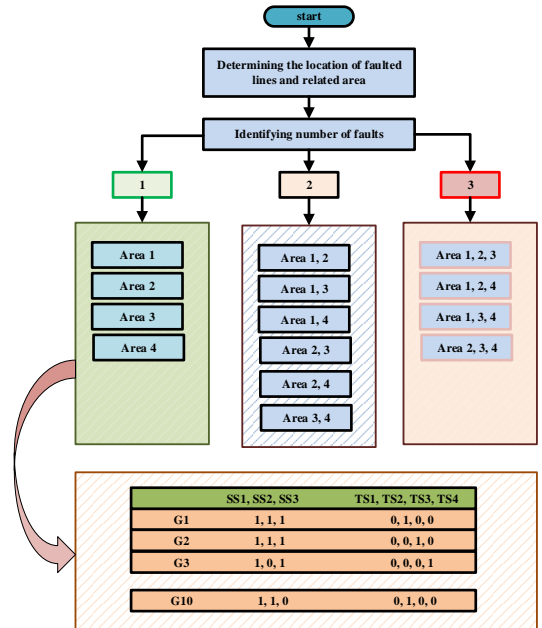


Fig. 1. Database of the DFR topologies.

Fig. 1. Database of the DFR topologies.

2.5. Constraints of DERs and MG

The constraints formulated for the proposed model are outlined as follows:

• Constraints of DERs

DERs are considered as PVs and MTs in this paper. The restrictions of generation push MTs that run such that meet the number of technical limitations. These boundaries encompass smallest and highest capacity, and up/down ramping rates [31, 32]. To assure that the planned electrical power in each phase of MT considers its smallest and highest capacity constraints, Eq. (5) is depicted as follows [31, 32]:

$$P^{min}(g) \leq P^{MT}(g, t, \varphi) \leq P^{max}(g) \quad (5a)$$

$$\forall g \in N_{MT}, t \in T, \varphi \in N_{ph}$$

$$P^{MT}(g, t, \varphi) - P^{MT}(g, t-1, \varphi) \leq RP^{RU}(g) \quad (5b)$$

$$\forall g \in N_{MT}, t \in T, \varphi \in N_{ph}$$

$$P^{MT}(g, t-1, \varphi) - P^{MT}(g, t, \varphi) \leq RP^{RD}(g) \quad (5c)$$

$$\forall g \in N_{MT}, t \in T, \varphi \in N_{ph}$$

The detail of constraint Eq. (5) is as follows: Eq. (5a) determines the maximum and minimum capacity of MTs. Eqs. (5b) and Eq. (5c) clarify the boundaries of ramp-up and ramp-down [32, 33].

• Constraints of DRP

For each phase of demand, the value of demand reduction should not surpass the upper limit if this demand can be delivered by the tie line. The DRP contract determines this upper limit [30].

$$0 \leq P^{DR}(d, t, \varphi) \leq P^{DR, max}(d, t) \quad (6)$$

$$\forall d \in N_L, t \in T, \varphi \in N_{ph}$$

The power factor of loads is considered a constant value. Consequently, the reactive power variables can be substituted by the active power variables as follows [27]:

$$Q^{DR}(d, t, \varphi) = \lambda(d, \varphi) \times P^{DR}(d, t, \varphi) \quad (7)$$

$$\forall d \in N_L, t \in T, \varphi \in N_{ph}$$

• RER generation

The output power of each phase of RERs that are PVs in this paper is limited as follows [33]:

$$0 \leq P^{RER}(r, t, \varphi) \leq P^{RER, max}(r, t) \quad (8a)$$

$$\forall r \in RE, t \in T, \varphi \in N_{ph}$$

It is assumed that PV panels operate at the maximum power point tracking. It is clear that the output power of PV panels is proportional to solar irradiance. Correspondingly, datasheets of the manufacturers denote that if solar irradiance of a PV cell equals 1000 w/m^2 , its maximum output power will be happened. However, if the solar irradiance surpasses this amount, the output of the PV cell still equals the rated capacity [34].

$$P^{RER}(r, t, \varphi) = \begin{cases} Irr(t) \times P^{RER, max}(r, t) & \text{if } Irr(t) \leq 1000 \\ P^{RER, max}(r, t) & \text{if } Irr(t) > 1000 \end{cases} \quad (8b)$$

$$\forall r \in RE, t \in T, \varphi \in N_{ph}$$

• Network constraints

The electrical power in each phase of buses which is connected to at least one line that has $s_l = 1$ in MG is balanced as [35]:

$$P^{RER}(t, i, \varphi) + P^{MT}(t, i, \varphi) - (P^L(t, i, \varphi) - P^{DR}(t, i, \varphi)) = \sum_{\forall j \in N_{bus}} [g(i, j, \varphi) \times v(t, i, \varphi) \times v(t, j, \varphi)] \quad (9a)$$

$$\forall t \in T, \forall \varphi \in N_{ph}, \forall i \in N_{bus}, \forall (i, j) \in G(k)$$

$$Q^{cap}(t, i, \varphi) - (Q^L(t, i, \varphi) - Q^{DR}(t, i, \varphi)) = \sum_{\forall j \in N_{bus}} [b(i, j, \varphi) \times v(t, i, \varphi) \times v(t, j, \varphi)] \quad (9b)$$

$$\forall t \in T, \forall \varphi \in N_{ph}, \forall i \in N_{bus}, \forall (i, j) \in G(k)$$

Where $Q^{cap}(t, i, \varphi)$ is calculated as follows:

$$Q^{cap}(t, i, \varphi) = Q_{rated}^{cap}(i, \varphi) \times v^2(t, i, \varphi) \cong Q_{rated}^{cap}(i, \varphi) \times [2 \times v(t, i, \varphi) - 1] \quad (9c)$$

$$\forall t \in T, \forall \varphi \in N_{ph}, \forall i \in N_{cap}$$

To adjust the protection issues, the succeeding restrictions are treated on feeder currents and bus voltages for the MG operation [35]:

$$V^{Min} \leq v(t, i, \varphi) \leq V^{Max} \quad (9d)$$

$$\forall t \in T, \forall \varphi \in N_{ph}, \forall i \in N_{bus}$$

$$-f^{Max}(i, j, \varphi) \leq f(t, i, j, \varphi) \leq f^{Max}(i, j, \varphi) \quad (9e)$$

$$\forall t \in T, \forall i, j \in N_{bus}, \forall \varphi \in N_{ph}, \forall (i, j) \in G(k)$$

$$f(t, i, j, \varphi) = [v(t, i, \varphi) \times (v(t, i, \varphi) - v(t, j, \varphi)) \times g(i, j, \varphi)] + [v(t, i, \varphi) \times (v(t, i, \varphi) - v(t, j, \varphi)) \times b(i, j, \varphi)]$$

It is realized that the anticipated model is a non-convex nonlinear model, because Eq. (9) is a non-affine equality constraint. Thus, using conformist optimization algorithms cannot certify harvesting globally optimal solutions. Furthermore, for real-time applications, a fast and consistent algorithm is needed. To achieve this goal, it is better to linearize power flow constraints. If equations are linearized, LPF-D will calculate the magnitude and phase angle of bus voltages simultaneously with high accuracy [36]. To conclude, all equations are linear or linearized by the method proposed by [27] and the whole optimization is a MILP problem.

2.6. Estimation of the probability of line fault

The aim of the proposed OMS is the minimization of the operating cost within outages and energy not supplied $N - K$ contingencies due to extreme weather events, for example, hurricanes. Evaluation of the probability of occurrence of $N - K$ contingencies is necessary until the maximum K considered by MGO is determined. It is seen that for $K > 3$, $N - K$ contingencies have a probability of very small [27, 37]. Consequently, this paper takes into $N - 1$, $N - 2$, and $N - 3$ contingencies consideration for the demonstration of the OMS.

3. ROBUST OPTIMIZATION METHOD

Different optimization methods can handle uncertainties. For example, probabilistic optimization, stochastic programming, interval optimization, and robust optimization [38]. It can be noted that the latter is very well-known for scholars and planners because of its prevailing risk management, high robustness, and low computational load [38]. It can be noted that the most important advantage of robust optimization in comparison with other approaches is the lack of need for PDF or membership functions of the uncertain inputs [39].

The succeeding equations depict a typical LP optimization model as [39]:

$$\text{Min} \sum_{n \in N} d(n) \times x(n) \quad (10)$$

Subject to:

$$\sum_{n \in N} e(m, n) \times x(n) \leq f(m) \quad \forall m \in M \quad (11a)$$

$$lx(n) \leq x(n) \leq ux(n) \quad \forall n \in N \quad (11b)$$

$$x(n) \in Z; \forall n = 1, 2, \dots, k \text{ and } x(n) \in R; \forall n = k + 1, k + 2, \dots \quad (11c)$$

This approach considers limited intervals to model the input uncertainties. These intervals are determined concerning sets of uncertainties. Thereby, $d(n)$ and $e(m, n)$ as the uncertain elements are written as follows:

$$d(n) = [\bar{d}(n) - \hat{d}(n), \bar{d}(n) + \hat{d}(n)] \quad \forall n \in N \quad (12a)$$

$$e(m, n) = [\bar{e}(m, n) - \hat{e}(m, n), \bar{e}(m, n) + \hat{e}(m, n)] \quad \forall n \in N, \forall m \in M \quad (12b)$$

The proposed RLP problem is formulated by introducing an integer parameter $\beta(m)$ which controls the conservation level and it belongs to the interval $[0, |J(m)|]$. Surely, $J(m)$ is set of uncertain elements of not only the objective function ($m = 0$) that is $J(0) = \{n | d(n) > 0\}$ but also the restriction m that is $J(m) = \{n | e(m, n) > 0\}$ [40]. Considering that all the uncertain elements cannot deviate from their nominal values at the same time, this paper assumes that up to $\beta(m)$ of these variables can change within specified intervals defined by Eq. (12), although the deviation of one of them is circumscribed by subsequent reduced intervals [40]:

$$\begin{aligned} dt(0) &= [\bar{dt}(0) - (\beta(0) - \beta(0)) \times \hat{dt}(0), \\ \bar{dt}(0) + (\beta(0) - \beta(0)) \times \hat{dt}(0)] \\ \forall dt(0) \in J(0), m = 0 \end{aligned} \quad (13a)$$

$$\begin{aligned} et(m, n) &= [\bar{et}(m, n) - (\beta(m) - \beta(m)) \times \hat{et}(m, n), \\ \bar{et}(m, n) + (\beta(m) - \beta(m)) \times \hat{et}(m, n)] \\ \forall et(m, n) \in J(m), \forall m \in M \end{aligned} \quad (13b)$$

It is clear that $\beta(m)$ is a real number. For instance, if $\beta(m)$ is equal to 2.5, it can be deduced that uncertain elements of two restrictions can change inside the complete range of the defined limits, although, uncertain elements of one of the restrictions have a disparity inside half range.

The RLP model of the suggested LP expressed as Eq. (1) is assumed as [39]:

$$\begin{aligned} &Min \sum_{n \in N} \bar{d}(n) \times x(n) + \\ &max_{\{\Psi(0) \cup \{\Theta(0)\} | \Psi(0) \subseteq J(0), \Psi(0) = \Upsilon(0), \Theta(0) \in J(0) / \Psi(0)\}} \times \\ &\left\{ \sum_{n \in \Psi(0)} \hat{d}(n) \times |x(n)| - \Upsilon(0) \right\} \times \hat{dt}(0) \times |xt(0)| \end{aligned} \quad (14)$$

Subjected to:

$$\begin{aligned} &\sum_{n \in N} \bar{e}(m, n) \times x(n) + \\ &max_{\{\Psi(m) \cup \{\Theta(m)\} | \Psi(m) \subseteq J(m), \Psi(m) = \Upsilon(m), \Theta(m) \in J(m) / \Psi(m)\}} \times \\ &\left\{ \sum_{n \in \Psi(0)} \hat{e}(m, n) \times |x(n)| + (\Upsilon(0) - \Upsilon(0)) \times \right. \\ &\left. \hat{et}(m, n) \times |xt(m)| \right\} \quad \forall m \in M \end{aligned} \quad (15)$$

Moreover, Eqs. (11b) and (11c)

The robust problem defined by Eqs. (14)- (15) and (11b) and (11c) is a robust nonlinear problem which is linearized by duality theory [33]. and consequently, the resulted RLP is written as [33]:

$$Min \sum_{n \in N} \bar{d}(n) \times x(n) + z(0) \times \beta(0) + \sum_{n \in J(0)} p(0, n) \quad (16)$$

Subjected to:

$$\sum_{n \in N} \bar{e}(m, n) \times x(n) + z(m) \times \beta(m) + \sum_{n \in J(m)} p(m, n) \leq f(m) \quad \forall m \in M \quad (17a)$$

$$z(0) + p(0, n) \geq \hat{d}(n) \times \theta(n) \quad \forall n \in J(0) \quad (17b)$$

$$z(m) + p(m, n) \geq \hat{e}(m, n) \times \theta(n) \quad \forall n \in J(m), \forall m \in M \quad (17c)$$

$$-\theta(n) \leq x(n) \leq \theta(n) \quad \forall n \in N \quad (17d)$$

$$lx(n) \leq x(n) \leq ux(n) \quad \forall n \in N \quad (17e)$$

$$p(m, n) \geq 0, \quad \forall n \in J(m), \forall m \in M \quad (17f)$$

$$\theta(n) \geq 0 \quad \forall n \in N \quad (17g)$$

$$z(m) \geq 0 \quad \forall m \in M \quad (17h)$$

$$\begin{aligned} x(n) &\in Z; \quad \forall n = 1, 2, \dots, k \text{ and} \\ x(n) &\in R; \quad \forall n = k + 1, k + 2, \dots \end{aligned} \quad (17i)$$

Thereby, Eqs. (1)- (9) in deterministic form can be reformulated by Eqs. (16)- (17) as follows:

$$Min (Cost(G(k))) \quad (18)$$

Subjected to:

$$0 \leq \bar{P}^{RER}(r, t, \varphi) \leq P^{RER, max}(r, t) \quad \forall r \in RE, t \in T, \varphi \in N_{ph} \quad (19a)$$

$$\begin{aligned} &\bar{P}^{RER}(t, i, \varphi) + P^{MT}(t, i, \varphi) - \\ &(\bar{P}^L(t, i, \varphi) - P^{DR}(t, i, \varphi)) = \\ &\sum_{\forall j \in N_{bus}} [g(i, j, \varphi) \times v(t, i, \varphi) \times v(t, j, \varphi)] \\ &\forall t \in T, \forall \varphi \in N_{ph}, \forall i \in N_{bus}, \forall (i, j) \in G(k) \end{aligned} \quad (19b)$$

$$(2) - (7) \text{ and } (9b) - (9e) \quad (19c)$$

$$\begin{aligned} &z^{RER}(r, t, \varphi) + p^{RER}(r, t, \varphi) \geq \\ &\bar{P}^{RER}(r, t, \varphi) \times \theta^{RER}(r, t, \varphi) \\ &\forall t \in T, r \in RE, \forall \varphi \in N_{ph} \end{aligned} \quad (19d)$$

$$\begin{aligned} &z^{PL}(d, t, \varphi) + p^{PL}(d, t, \varphi) \geq \\ &\bar{P}^L(d, t, \varphi) \times \theta^{PL}(d, t, \varphi) \\ &\forall t \in T, d \in D, \forall \varphi \in N_{ph} \end{aligned} \quad (19e)$$

$$\begin{aligned} &z^{RER}(r, t, \varphi) \geq 0; \\ &p^{RER}(r, t, \varphi) \geq 0; \\ &\theta^{RER}(r, t, \varphi) \geq 1 \\ &\forall t \in T, r \in RE, \forall \varphi \in N_{ph} \end{aligned} \quad (19f)$$

$$\begin{aligned} &z^{PL}(d, t, \varphi) \geq 0; \\ &p^{PL}(d, t, \varphi) \geq 0; \\ &\theta^{PL}(d, t, \varphi) \geq 1 \\ &\forall t \in T, d \in D, \forall \varphi \in N_{ph} \end{aligned} \quad (19g)$$

It can be noted that the non-linear terms in Eq. (19) will be linear by the duality theory. The indeterminate inputs i.e. electrical loads and renewable generations are demonstrated by symmetric limited intervals as follows [39]:

$$\begin{aligned} &p^{RER}(r, t, \varphi) = \\ &[P^{RER}(r, t, \varphi) - \bar{P}^{RER}(r, t, \varphi), P^{RER}(r, t, \varphi) + \bar{P}^{RER}(r, t, \varphi)] \\ &\forall t \in T, r \in RE, \forall \varphi \in N_{ph} \end{aligned} \quad (20a)$$

$$\begin{aligned} &p^{PL}(d, t, \varphi) = \\ &[P^L(d, t, \varphi) - \bar{P}^L(d, t, \varphi), P^L(d, t, \varphi) + \bar{P}^L(d, t, \varphi)] \\ &\forall t \in T, d \in D, \forall \varphi \in N_{ph} \end{aligned} \quad (20b)$$

The Eqs. (18)- (20) represent the anticipated RLP.

4. THE APPLICATION OF THE SOLUTION ALGORITHM TO THE MATHEMATICAL MODEL

4.1. OMS considering DFR

In brief, the OMS wants to optimally determine the DFR to restore as much demand as possible under $N - K$, ($K \leq 3$) contingencies. Fig. 2 briefly shows the proposed OMS strategy. During the occurrence of a line fault, the MGO carries out the faulted line location and then determines the area which includes this line. Afterward, the MGO looks up the related topology Eq. (4a) in the provided database shown in Fig. 1. Then, the MGO obtains the incidence matrix for each topology and computes its rank. The LP pertaining to DER scheduling will be solved given the rank is $N - 1$. For topologies that are isolated or that have infeasible solutions, the proposed graph is ignored. Finally, the MGO chooses the optimal topology after scanning all of the DFRs.

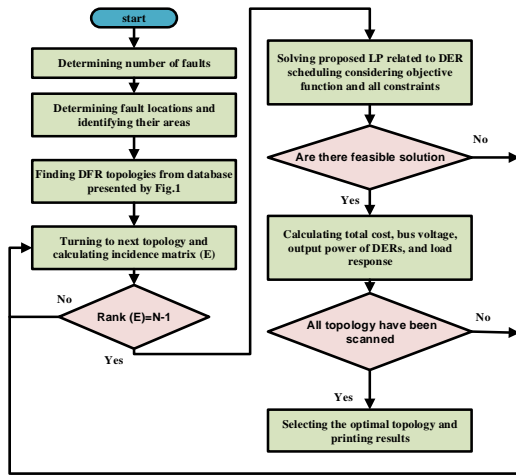


Fig. 2. The proposed OMS strategy.

Fig. 2. The proposed OMS strategy.

The suggested model is solved by a GAMS-based solver that is CPLEX 12.1 with a MIP gap of 0.1%. this solver has an appropriate efficacy to solve LP problems [41]. PC utilized for running simulations has appropriate structures including Intel Core i7, 2.5GHz CPU with 12 GB of RAM.

5. SIMULATION RESULTS

An outage may happen at any MG line when there is a severe weather condition for example hurricanes. This section presents simulation results on the modified IEEE 69-bus unbalanced test system.

5.1. The under-study system

The modified 69-bus unbalanced MG illustrated in Fig. 3 is treated as a test system that evaluates the efficacy of the advised model. The test system has three MTs, seven PVs, three critical SSs, four TSs, and four SCs. To increase the probability of volt-age violation, each electrical demand of the original 69-bus test system is multiplied by 2.0. This assumption makes an opportunity that the robustness of the proposed OMS to be checked. Also, to make unbalance in feeders, it is assumed that in Fig. 3, Sections 24-25, 25-26, and 64-65 are two phases, and Sections 51-52, and 68-69 are single phases. Table 1 denotes the parameters of the under-study system. Figs. 4 and 5 present forecasted electrical demands together with solar irradiance of PVs, respectively.

Table 1. The characteristics of under study system [27].

Parameter	Value	Parameter	Value
C^{MT} (\$/kWh)	0.25	C^L (\$/kWh)(for critical load)	12
λ	0.71	C^L (\$/kWh)(for non-critical load)	0.4
Q_{rated}^{cap} (kVAr)	1400	P^L (kW) for peak	7.58
P^{max} (kW)	1160	P^{min} (kW)	0
$RPRD$ (kW/h)	400	$RPRU$ (kW/h)	400
$P^{DR,max}$ (kW)	$0.3P^L$	$P^{RER,max}$ (kW)	1200
V^{Min} (pu)	0.92	V^{Max} (pu)	1.05
V^{sub} (pu)	1.03	S^{base} (kVA)	8000
V^{base} (kV)	12.47		

5.2. Sensitivity analysis

The sensitivity of the objective functions to the amount of uncertainty of input parameters is analyzed in this subsection. These studies have been illustrated in Fig. 6. To better evaluate, two studies is treated as:

- **Study 1:** handling uncertainty of electrical loads,
- **Study 2:** handling uncertainty of PV generations.

The horizontal axis of Fig. 6 reflects the variation of the control parameter of the uncertainty. It is seen, this parameter changes in the range zero up to one by steps 0.1. The uncertainty parameter is zero when the decisions are made without consid-ering risk i.e., risk-neutral and it is one when the decisions are made based on risk-averse. Fig. 6 says to us, that if decisions of MGOs make based on high risk-averse, the cost will rise for two studies. To put it more simply, the more the uncertainty of pa-rameters, the more the operating cost is. It can be noted that increasing uncertainty of electrical loads is to increase electrical demands from the anticipated values and increasing uncertainty of RER generations is to decrease RER productions from the anticipated amounts. With rising the uncertainty parameter from 0 to 1 in Study 1 and 2, the cost is rising by 38.39%, and 28.80%, respectively. As well, Fig. 6 signifies that the effect of uncertainty in electrical demand is more than uncertainty in RER generation on increasing cost.

5.3. Case studies

To measure the competence of the proposed model, the two following case studies are considered. The stochastic behavior of demands and RERs are modeled considering a moderate value for the uncertainty parameter that is 0.5.

A) Case study of double contingencies

In this subsection, the paper deals with two following extreme scenarios of $N - 2$ contingencies:

- **Scenario 1:** Lines 10–11 and 54–55 are faulted and faults are cleared at 13:00.
- **Scenario 2:** Lines 12–13 and 47–48 are faulted and faults are cleared at 13:00.

Table 2 shows the resulted topologies for the two above-mentioned scenarios. It can be noted that the burden time of Scenarios 1 and 2 are 188 and 215 seconds, respectively. Regarding Table 2, ten and nine topologies are nominated for Scenarios 1 and 2, respectively. The optimal topologies in Scenarios 1 and 2 are $G(9)$ and $G(7)$ that have minimum costs of 5734 (\$) and 5945 (\$), respectively. However, some topologies in the first scenario that are $G(2)$, $G(4)$, $G(5)$, and $G(6)$ cannot result in feasible solutions and they should be ignored. Also, some topologies in the second scenario that are $G(1)$, $G(4)$, $G(5)$, $G(6)$, and $G(9)$ are omitted by the rank constraint due to having non-connected graphs. Fig. 7 shows the optimal DFR topologies of the two studied scenarios.

Figs. 8 and 9 show the total MTs generation and the total amount of load reduction at each hour. It is seen that although total MT generations and the total amount of load reduction have close patterns in both scenarios, the cost of Scenario 2 is 3.6% more than Scenario 1. The cause of higher cost is to turn off

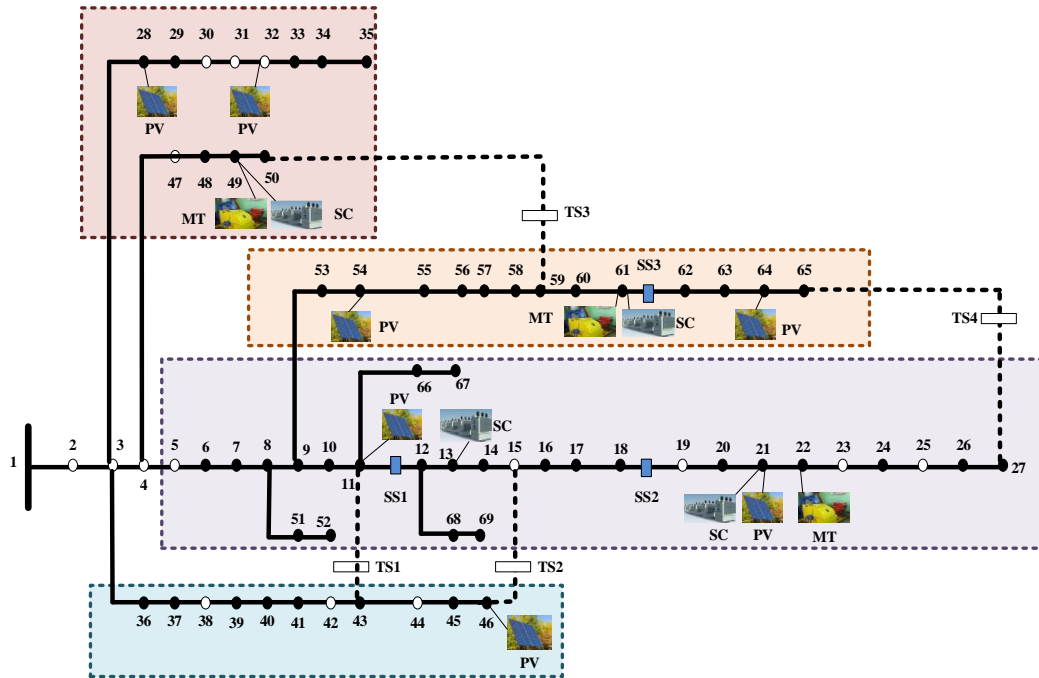


Fig. 3. The modified 69-bus unbalanced test system.

Table 2. The resulted topologies for Scenarios 1 and 2.

G(k)	Scenario 1		Scenario 2	
	Actions	Total cost (\$)	Actions	Total cost (\$)
G(1)	Closing TS3 and TS1	6410	Closing TS3 and TS1	Non-connected
G(2)	Closing TS4 and TS1	Non-feasible	Closing TS3 and TS2	7689
G(3)	Closing TS3 and TS2	6407	Closing TS4 and TS3	8879
G(4)	Closing TS4 and TS2	Non-feasible	Closing TS4, TS1, and TS3, Opening SS1	Non-connected
G(5)	Closing TS4 and TS3	Non-feasible	Closing TS4, TS1, and TS3, Opening SS2	Non-connected
G(6)	Closing TS4, TS1 and TS3, Opening SS1	Non-feasible	Closing TS4, TS1, and TS3, Opening SS3	Non-connected
G(7)	Closing TS4, TS1 and TS3, Opening SS2	5823	Closing TS4, TS2, and TS3, Opening SS2	5945
G(8)	Closing TS4, TS1 and TS3, Opening SS3	7894	Closing TS4, TS2, and TS3, Opening SS3	6987
G(9)	Closing TS4, TS2 and TS3, Opening SS2	5734	Closing TS3, TS1, and TS2, Opening SS1	Non-connected
G(10)	Closing TS4, TS2 and TS3, Opening SS3	7409		

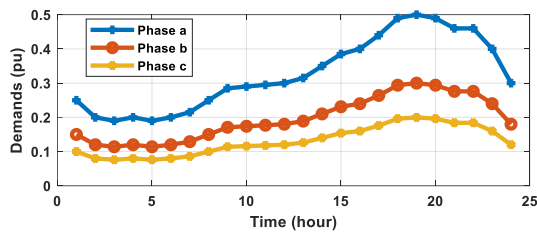


Fig. 4. The prophisied electrical loads for each hour in the day ahead [42].

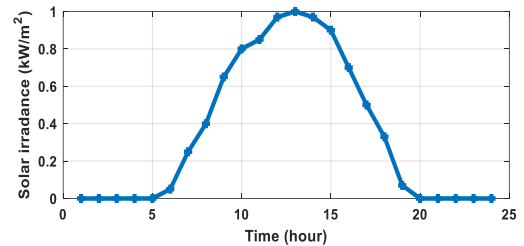


Fig. 5. The prophisied electrical power produced by RER (PVs) [27].

more critical demands in Scenario 2. Fig. 8 shows that the load reductions in each phase are maximized at hour 19. The load reduction of Scenario 1 for phases a, b, and c at hour 19 is 1.95 MW, 1.17 MW, and 0.78 M, respectively. Simulation results of Scenario 2 depict that if the islanded loads are only supplied by MTs and PVs with considering DFR, the amount of total load decrease for phases a, b, and c at the same hour will be 2 MW, 1.2 MW, and 0.8 MW, respectively that it totally is 2.5% more than scenario 1.

Fig. 10 shows the minimum voltage of all buses in each phase

and at each hour. It is seen that some buses are faced with unacceptable voltage drops during peak hours in Scenario 2. This problem is triggered by heavy loading of lines 57–58, 60–61, and 63–64 that have high impedance. It is worthwhile to note that during normal operation, there is a voltage drop problem when the MG tolerates the heavy loading. It can be noted that keeping the bus voltages between admissible thresholds is not vital for MGO during the outage period, while the highest priority for MGO is to serve more loads during this period. Thereby, the voltage constraints of the proposed model can be relaxed to serve more

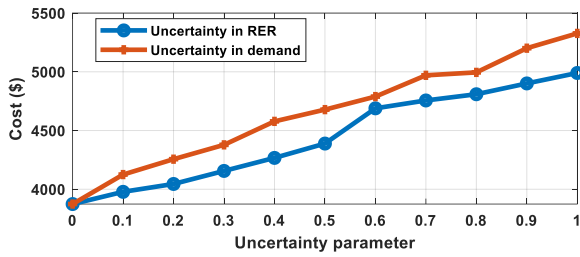


Fig. 6. Effect of vagueness on the cost.

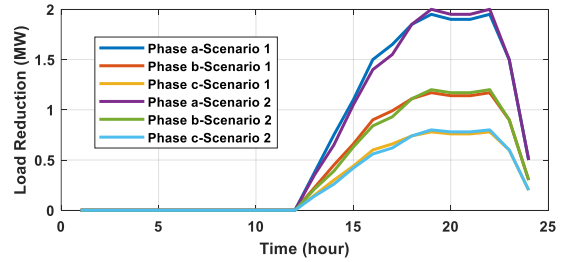


Fig. 9. The total load reduction.

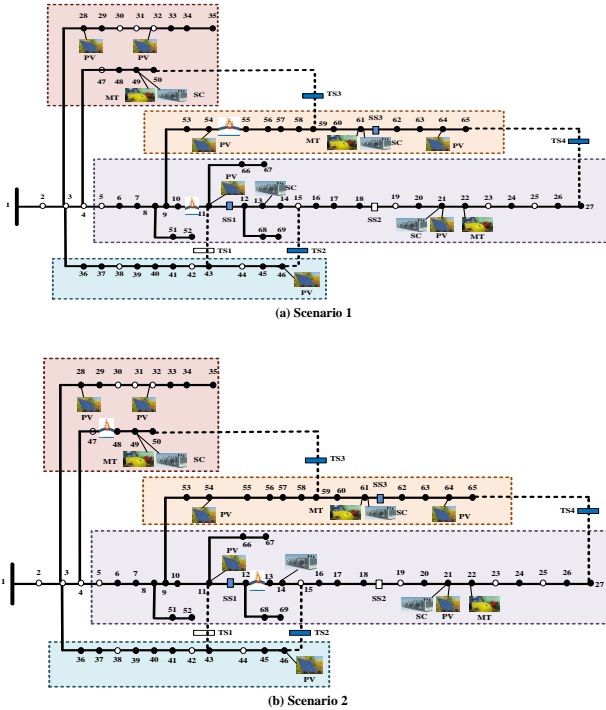
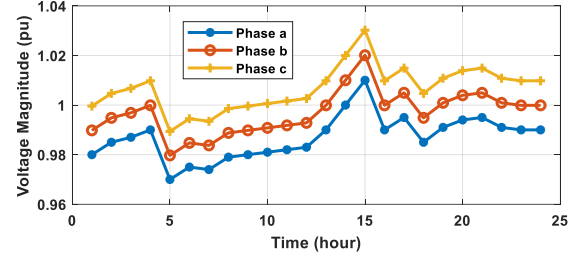
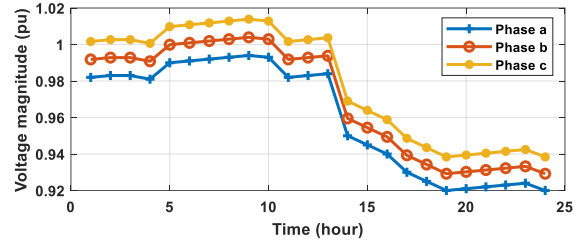


Fig. 7. Optimal DFR topologies.



(a) Scenario 1



(b) Scenario 2

Fig. 10. The voltage profile.

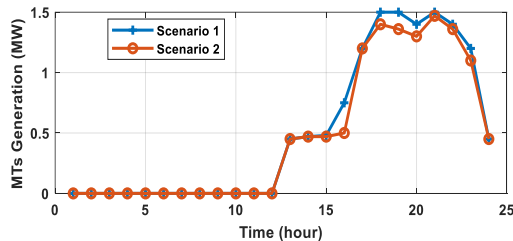


Fig. 8. The total MTs generation.

demands. As well, the shunt capacitors may be installed by MGO adjacent to the large demands to enhance voltage profiles. To sum up briefly, the bus voltage constraints should be re-laxed to decrease or even reject the load reduction because of voltage drop during doing DFR.

B) Case study of triple contingencies

In this subsection, the paper considers two succeeding drastic scenarios of $N - 3$ contingencies:

- **Scenario 3:** Lines 12–13, 38–39, and 4–47 are faulted and faults are cleared at 13:00.
- **Scenario 4:** Lines 36–37, 47–48, and 62–63 are faulted and faults are cleared at 13:00.

Table 3 shows the final topologies for the two aforementioned scenarios. It can be noted that the computation time of Scenarios 3 and 4 are 145 and 177 seconds, respectively. Regarding Table 3, four and five topologies are selected for Scenarios 3 and 4, respectively. The optimal topologies in Scenarios 3 and 4 are $G(4)$ and $G(1)$ that have minimum costs of 8679 (\$) and 6789 (\$), respectively. Nevertheless, one topology in the first scenario that is $G(3)$ and two topologies in the second scenario that are $G(4)$, and $G(5)$ are lost by the rank restriction because of having non-connected graphs. Fig. 11 displays the optimal DFR topologies of Scenarios 3 and 4.

Figs. 12 and 13 display the total MTs generation and the total amount of load reduction at each hour. It can be observed while total MTs generation and the total amount of load reduction have similar variations in both scenarios, the cost of Scenario 3 is 27.8% more than Scenario 4. The reason for the higher cost is to turn off more critical demands in Scenario 3. Fig. 12 shows that the load reductions in each phase are the highest value at hour 19. The load reduction for phases a, b, and c at hour 19 is 1.9 MW, 1.14 MW, and 0.76, respectively. Simulation results represent that if the isolated demands are only served by MTs and PVs barring DFR, the amount of total load reduction for phases a, b, and c at the same hour will be 2.05 MW, 1.23 MW, and 0.82, respectively that it totally is 7.8% more than scenario 3. Consequently, DFR has significantly decreased the load reduction even when the penetration of the DER is relatively low.

Table 3. The resulted topologies for Scenarios 3 and 4.

G(k)	Scenario 3		Scenario 4	
	Actions	Total cost (\$)	Actions	Total cost (\$)
G(1)	Closing TS4, TS1, and TS3	9567	Closing TS4, TS1, and TS3	6789
G(2)	Closing TS4, TS2, and TS3	9879	Closing TS4, TS2, and TS3	6834
G(3)	Closing TS3, TS1, TS2, and TS4, Opening SS1	Non-connected	Closing TS3, TS1, TS2, and TS4, Opening SS1	7345
G(4)	Closing TS3, TS1, TS2, and TS4, Opening SS2	8679	Closing TS3, TS1, TS2, and TS4, Opening SS2	Non-connected
G(5)			Closing TS3, TS1, TS2, and TS4, Opening SS3	Non-connected

Table 4. Assessment of outcomes of proposed and deterministic model for different scenarios.

Model	Scenario 1 (\$)			Scenario 2 (\$)			Scenario 3 (\$)			Scenario 4 (\$)		
	Objective func-	Time of conver-										
Proposed	5734	184	5945	467	8679	203	6789	588				
Deterministic	5134	135	5356	380	8143	178	5981	507				

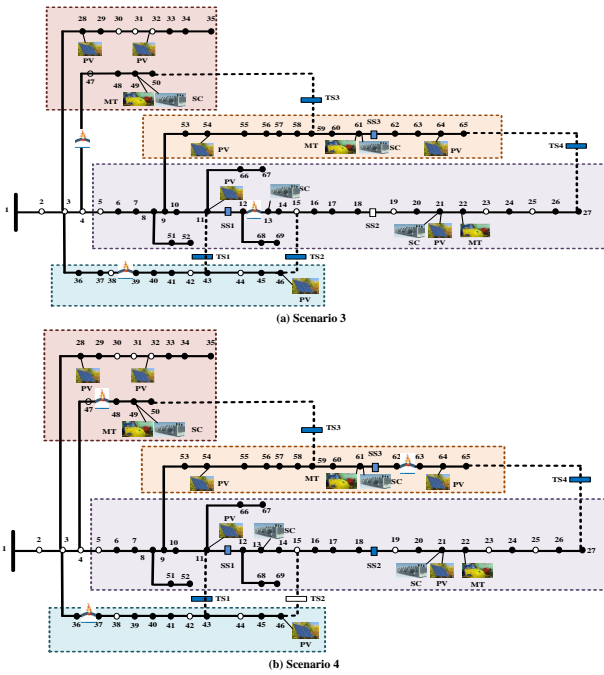


Fig. 11. Optimal DFR topologies.

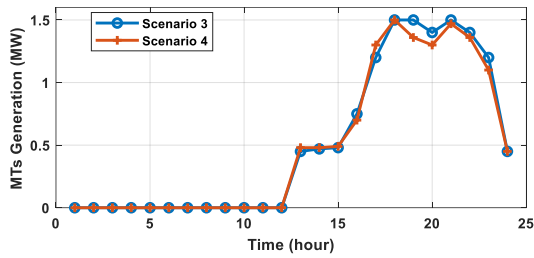


Fig. 12. The total MTs generation.

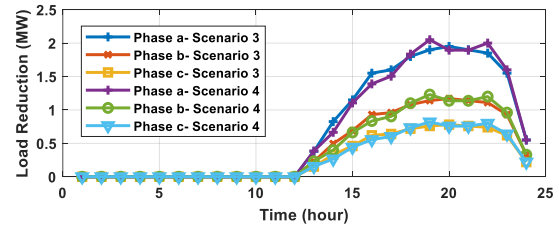
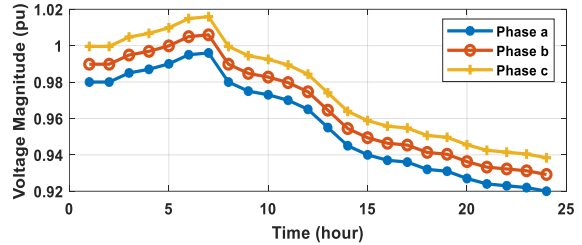
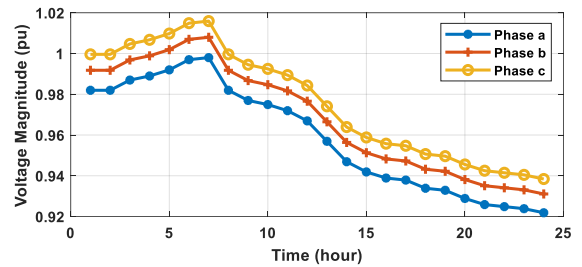


Fig. 13. The total load reduction.



(a) Scenario 3



(b) Scenario 4

Fig. 14. The voltage profile.

Fig. 14 shows the average of three phase voltages in each bus and at each hour. Like Scenario 2, the outcomes of Scenario 3 also specify that some demands are interrupted due to voltage restrictions. In addition, the bus voltage bounds should be re-relaxed, if is desirable, to decrease or even reject the load decrease because of voltage violation.

5.4. Comparison between models

A comparison between the proposed model and the deterministic model is done in this subsection for four scenarios. The objec-

function for four scenarios is derived from the proposed and the deterministic model (Table 4). Regarding this table, the proposed model has a final objective function of 11.6% more than the deterministic model and an execution time of 36.2% more than the deterministic model in Scenario 1. In addition, in Scenario 2, the final objective function and execution time in the proposed model are 10.9% and 22.8% more than the deterministic model, respectively. The above-mentioned values are 6.5% and 14.04% in Scenario 3 and 13.5% and 15.90% in Scenario 4.

6. CONCLUSION AND FUTURE WORK

A resilient DN means supplying as much demand as possible after $N - K$ contingencies respond to natural disasters. A robust OMS for the post-fault restoration of DN is developed by this paper with considering the stochastic behavior of electrical demands and solar irradiance. The proposed OMS includes both DFR and DER scheduling. Unlike MG-based restoration methods that need a high DER penetration level, the proposed model is appropriate to be applied to those DNs that have numerous TSs and low DER penetration level. This paper has two key contributions. Firstly, the selection of an optimal topology to minimize the total cost of the outage based on rank-based restrictions to guarantee the radial structure. Secondly, proposing an optimal DER scheduling model with taking into account DERs including dispatchable MTs, non-dispatchable PVs, SCs, and DRP. The presented model is tested by the different scenarios which study the severe electrical power outage and low solar irradiance. The simulation results specify that the suggested approach can preserve a high proportion of demands in service in storm days which $N - 2$ and $N - 3$ contingencies are very common. To conclude, using the proposed model averagely increases total operation cost and execution time by 10.62% and 22.23% on all scenarios compared to the deterministic model. It is observed that even though the proposed model is not a less expensive and quick method to work out optimal OM in comparison to deterministic ones, the proposed model solutions are more realistic for the real world. Modeling solar irradiance pattern as dissimilar in the DN, modeling PV operating cost, and operating the MTs and PVs under the non-unity power factors for supporting voltage and reactive power can be considered future works.

REFERENCES

- [1] A. Dehghani, M. Sedighzadeh, and F. Haghjoo, "An overview of the assessment metrics of the concept of resilience in electrical grids," *Int. Trans. Electr. Energy Syst.*, vol. 31, no. 12, p. e13159, 2021.
- [2] S. Behzadi, A. Bagheri, and A. Rabiee, "Resilience-oriented operation of micro-grids in both grid-connected and isolated conditions within sustainable active distribution networks," *J. Oper. Autom. Power Eng.*, 2023.
- [3] M. Abdelmalak and M. Benidris, "Proactive generation redispatch to enhance power system resilience during hurricanes considering unavailability of renewable energy sources," *IEEE Trans. Ind. Appl.*, vol. 58, no. 3, pp. 3044–3053, 2022.
- [4] N. Afsari, S. SeyedShenava, and H. Shayeghi, "A milp model incorporated with the risk management tool for self-healing oriented service restoration," *J. Oper. Autom. Power Eng.*, vol. 12, no. 1, pp. 1–13, 2024.
- [5] F. Jabari, M. Zeraati, M. Sheibani, and H. Arasteh, "Robust self-scheduling of pvs-wind-diesel power generation units in a standalone microgrid under uncertain electricity prices," *J. Oper. Autom. Power Eng.*, vol. 12, no. 2, pp. 152–162, 2024.
- [6] Q. Shi, W. Liu, B. Zeng, H. Hui, and F. Li, "Enhancing distribution system resilience against extreme weather events: Concept review, algorithm summary, and future vision," *Int. J. Electr. Power Energy Syst.*, vol. 138, p. 107860, 2022.
- [7] S. Ma, B. Chen, and Z. Wang, "Resilience enhancement strategy for distribution systems under extreme weather events," *IEEE Trans. Smart Grid*, vol. 9, no. 2, pp. 1442–1451, 2016.
- [8] Y. Lin and Z. Bie, "Tri-level optimal hardening plan for a resilient distribution system considering reconfiguration and dg islanding," *Appl. Energy*, vol. 210, pp. 1266–1279, 2018.
- [9] M. Sedighzadeh, M. Ghalambor, and A. Rezazadeh, "Reconfiguration of radial distribution systems with fuzzy multi-objective approach using modified big bang-big crunch algorithm," *Arabian J. Sci. Eng.*, vol. 39, pp. 6287–6296, 2014.
- [10] M. Sedighzadeh, G. Shaghghi-shahr, M. Esmaili, and M. R. Aghamohammadi, "Optimal distribution feeder reconfiguration and generation scheduling for microgrid day-ahead operation in the presence of electric vehicles considering uncertainties," *J. Energy Storage*, vol. 21, pp. 58–71, 2019.
- [11] Z. Wang and J. Wang, "Self-healing resilient distribution systems based on sectionalization into microgrids," *IEEE Trans. Power Syst.*, vol. 30, no. 6, pp. 3139–3149, 2015.
- [12] H. Farzin, M. Fotuhi-Firuzabad, and M. Moeini-Aghtaie, "Enhancing power system resilience through hierarchical outage management in multi-microgrids," *IEEE Trans. Smart Grid*, vol. 7, no. 6, pp. 2869–2879, 2016.
- [13] S. Ma, L. Su, Z. Wang, F. Qiu, and G. Guo, "Resilience enhancement of distribution grids against extreme weather events," *IEEE Trans. Power Syst.*, vol. 33, no. 5, pp. 4842–4853, 2018.
- [14] M. Sedighzadeh, M. Esmaili, and M. Mahmoodi, "Reconfiguration of distribution systems to improve reliability and reduce power losses using imperialist competitive algorithm," *Iran. J. Electr. Electron. Eng.*, vol. 13, no. 3, p. 287, 2017.
- [15] H. Farzin, M. Fotuhi-Firuzabad, and M. Moeini-Aghtaie, "Role of outage management strategy in reliability performance of multi-microgrid distribution systems," *IEEE Trans. Power Syst.*, vol. 33, no. 3, pp. 2359–2369, 2017.
- [16] C. Chen, J. Wang, F. Qiu, and D. Zhao, "Resilient distribution system by microgrids formation after natural disasters," *IEEE Trans. Smart Grid*, vol. 7, no. 2, pp. 958–966, 2015.
- [17] Y. Wang, Y. Xu, J. He, C.-C. Liu, K. P. Schneider, M. Hong, and D. T. Ton, "Coordinating multiple sources for service restoration to enhance resilience of distribution systems," *IEEE Trans. Smart Grid*, vol. 10, no. 5, pp. 5781–5793, 2019.
- [18] B. Chen, Z. Ye, C. Chen, and J. Wang, "Toward a milp modeling framework for distribution system restoration," *IEEE Trans. Power Syst.*, vol. 34, no. 3, pp. 1749–1760, 2018.
- [19] S. Yao, T. Zhao, P. Wang, and H. Zhang, "Resilience-oriented distribution system reconfiguration for service restoration considering distributed generations," in *2017 IEEE Power Energy Soc. Gen Meet.*, pp. 1–5, IEEE, 2017.
- [20] J. Liu, C. Qin, and Y. Yu, "Enhancing distribution system resilience with proactive islanding and rcs-based fast fault isolation and service restoration," *IEEE Trans. Smart Grid*, vol. 11, no. 3, pp. 2381–2395, 2019.
- [21] D. Dwivedi, P. K. Yemula, and M. Pal, "Evaluating the planning and operational resilience of electrical distribution systems with distributed energy resources using complex network theory," *Renewable Energy Focus*, 2023.
- [22] A. Rahiminejad, M. Ghafouri, R. Atallah, W. Lucia, M. Debbabi, and A. Mohammadi, "Resilience enhancement of islanded microgrid by diversification, reconfiguration, and der placement/sizing," *Int. J. Electr. Power Energy Syst.*, vol. 147, p. 108817, 2023.
- [23] A. Serrano-Fontova, Z. Liao, H. Li, and C. Booth, "A novel resilience assessment for active distribution networks including a der voltage regulation scheme considering windstorms," *Int. J. Electr. Power Energy Syst.*, vol. 153, p. 109310, 2023.
- [24] E. Kianmehr, S. Nikkhal, V. Vahidinasab, D. Giaouris, and P. C. Taylor, "A resilience-based architecture for joint distributed energy resources allocation and hourly network reconfiguration," *IEEE Trans. Ind. Inf.*, vol. 15, no. 10, pp. 5444–5455, 2019.
- [25] M. Sedighzadeh, G. Shaghghi-shahr, M. R. Aghamohammadi, and M. Esmaili, "A new optimal operation framework for balanced microgrids considering reconfiguration and

- generation scheduling simultaneously,” *Int. Trans. Electr. Energy Syst.*, vol. 30, no. 4, p. e12302, 2020.
- [26] G. Shaghaghi-shahr, M. Sedighzadeh, M. Aghamohammadi, and M. Esmaili, “Optimal generation scheduling in microgrids using mixed-integer second-order cone programming,” *Eng. Optim.*, vol. 52, no. 12, pp. 2164–2192, 2020.
- [27] Q. Shi, F. Li, M. Olama, J. Dong, Y. Xue, M. Starke, C. Winstead, and T. Kuruganti, “Network reconfiguration and distributed energy resource scheduling for improved distribution system resilience,” *Int. J. Electr. Power Energy Syst.*, vol. 124, p. 106355, 2021.
- [28] M. Sedighzadeh, S. S. Fazlhashemi, H. Javadi, and M. Taghvaei, “Multi-objective day-ahead energy management of a microgrid considering responsive loads and uncertainty of the electric vehicles,” *J. Cleaner Prod.*, vol. 267, p. 121562, 2020.
- [29] S. S. Fazlhashemi, M. Sedighzadeh, and M. E. Khodayar, “Day-ahead energy management and feeder reconfiguration for microgrids with cchp and energy storage systems,” *J. Energy Storage*, vol. 29, p. 101301, 2020.
- [30] P. Harsh and D. Das, “Optimal coordination strategy of demand response and electric vehicle aggregators for the energy management of reconfigured grid-connected microgrid,” *Renewable Sustainable Energy Rev.*, vol. 160, p. 112251, 2022.
- [31] F. H. Aghdam, N. T. Kalantari, and B. Mohammadi-Ivatloo, “A chance-constrained energy management in multi-microgrid systems considering degradation cost of energy storage elements,” *J. Energy Storage*, vol. 29, p. 101416, 2020.
- [32] F. Bouffard and F. D. Galiana, “Stochastic security for operations planning with significant wind power generation,” in *2008 IEEE Power Energy Soc. Gener. Meet.-Convers. Delivery Electr. Energy 21st Century*, pp. 1–11, IEEE, 2008.
- [33] Z. Tang, Y. Liu, L. Wu, J. Liu, and H. Gao, “Reserve model of energy storage in day-ahead joint energy and reserve markets: A stochastic uc solution,” *IEEE Trans. Smart Grid*, vol. 12, no. 1, pp. 372–382, 2020.
- [34] R. Torquato, Q. Shi, W. Xu, and W. Freitas, “A monte carlo simulation platform for studying low voltage residential networks,” *IEEE Trans. Smart Grid*, vol. 5, no. 6, pp. 2766–2776, 2014.
- [35] W. Gil-González, O. D. Montoya, E. Holguín, A. Garces, and L. F. Grisales-Noreña, “Economic dispatch of energy storage systems in dc microgrids employing a semidefinite programming model,” *J. Energy Storage*, vol. 21, pp. 1–8, 2019.
- [36] H. Yuan, F. Li, Y. Wei, and J. Zhu, “Novel linearized power flow and linearized opf models for active distribution networks with application in distribution Imp,” *IEEE Trans. Smart Grid*, vol. 9, no. 1, pp. 438–448, 2016.
- [37] S. Dunn, S. Wilkinson, D. Alderson, H. Fowler, and C. Galasso, “Fragility curves for assessing the resilience of electricity networks constructed from an extensive fault database,” *Nat. Hazard. Rev.*, vol. 19, no. 1, p. 04017019, 2018.
- [38] Z. K. Pecenek, M. Stadler, P. Mathiesen, K. Fahy, and J. Kleissl, “Robust design of microgrids using a hybrid minimum investment optimization,” *Appl. Energy*, vol. 276, p. 115400, 2020.
- [39] N. Rezaei, A. Khazali, M. Mazidi, and A. Ahmadi, “Economic energy and reserve management of renewable-based microgrids in the presence of electric vehicle aggregators: A robust optimization approach,” *Energy*, vol. 201, p. 117629, 2020.
- [40] N. Nikmehr, “Distributed robust operational optimization of networked microgrids embedded interconnected energy hubs,” *Energy*, vol. 199, p. 117440, 2020.
- [41] M. Kafaei, D. Sedighzadeh, M. Sedighzadeh, and A. S. Fini, “A two-stage igdt/tpem model for optimal operation of a smart building: A case study of gheshm island, iran,” *Therm. Sci. Eng. Prog.*, vol. 24, p. 100955, 2021.
- [42] S. M. Mousavi-Taghiabadi, M. Sedighzadeh, M. Zangiabadi, and A. S. Fini, “Integration of wind generation uncertainties into frequency dynamic constrained unit commitment considering reserve and plug in electric vehicles,” *J. Cleaner Prod.*, vol. 276, p. 124272, 2020.